Decomposition Controlled by Surface Morphology during Langmuir Evaporation of GaAs

J. Tersoff,[1,*] D. E. Jesson,[2,†] and W. X. Tang[2]

[1]*IBM T. J. Watson Research Center, Yorktown Heights, New York 10598, USA*
[2]*School of Physics, Monash University, Victoria 3800, Australia*
(Received 24 March 2010; published 14 July 2010)

When GaAs is heated in vacuum, it decomposes into Ga and As as it evaporates. Real-time *in situ* surface electron microscopy reveals striking bursts of ''daughter'' droplet nucleation and growth when coalescence of large ''parent'' droplets exposes nonplanar surface regions. We analyze the behavior, predicting a morphology-dependent congruent evaporation temperature. Based on this we propose a new approach for the self-assembly and positioning of quantum structures via droplet epitaxy, which we demonstrate at the proof-of-concept level.

DOI: 10.1103/PhysRevLett.105.035702 PACS numbers: 64.70.fm, 68.37.Nq, 68.43.Nr, 68.47.Fg

When GaAs is heated in vacuum, it evaporates by decomposing into Ga and As. Such Langmuir evaporation has been widely studied over the years, both for its fundamental scientific interest and for its technological importance in molecular beam epitaxy (MBE) growth and surface processing [1–8]. Above the congruent evaporation temperature T_c, the As evaporates preferentially, leaving behind Ga-rich liquid droplets [4–7]. Recently, the development of droplet epitaxy techniques has led to a resurgence of interest in such Ga droplets [9–13].

Here we apply real-time *in situ* surface electron microscopy to study the evaporation of GaAs (001). We find that Ga droplet formation is quite different than expected. Striking bursts of ''daughter'' droplet nucleation and growth occur in response to the coalescence of large ''parent'' droplets. We show that this unexpected behavior results from a strong coupling between morphology and evaporation. It is well known that evaporation can strongly influence morphology [14,15]. Here we also find the converse, that for GaAs the morphology dramatically affects the evaporation process. We conclude that the evaporation of As is controlled by step density, while evaporation of Ga is not. This leads to distinctive morphology effects in Langmuir evaporation of GaAs that have no analog in single-component systems such as Si. Analysis of these effects suggests a new approach for the self-assembly and positioning of quantum structures via droplet epitaxy, which we demonstrate at the proof-of-concept level. Our analysis moreover predicts that the congruent evaporation temperature T_c depends on morphology, consistent with our observations.

We degassed an undoped GaAs (001) $\pm 0.1°$ epi-ready wafer at 300 °C under ultrahigh vacuum for 24 h in a low energy electron microscope (Elmitec LEEM III) system. This was followed by high temperature flashing up to 600 °C and annealing at 580 °C for 2 h to remove the surface oxide. Ga droplets were produced by annealing at 650 °C, well above T_c. The base pressure of the system is below 2×10^{-10} Torr and typical pressures observed during imaging at annealing temperatures of 630 °C are in the range 7×10^{-9} Torr.

Figure 1 shows images from a photoemission electron microscopy (PEEM) video of Langmuir evaporation at 630 °C (available in the supplementary material [16]). Liquid Ga appears bright against dark GaAs due to relative work functions [17,18]. A typical snapshot displays droplets of very different size [Fig. 1(a)]. Past analyses [6] have

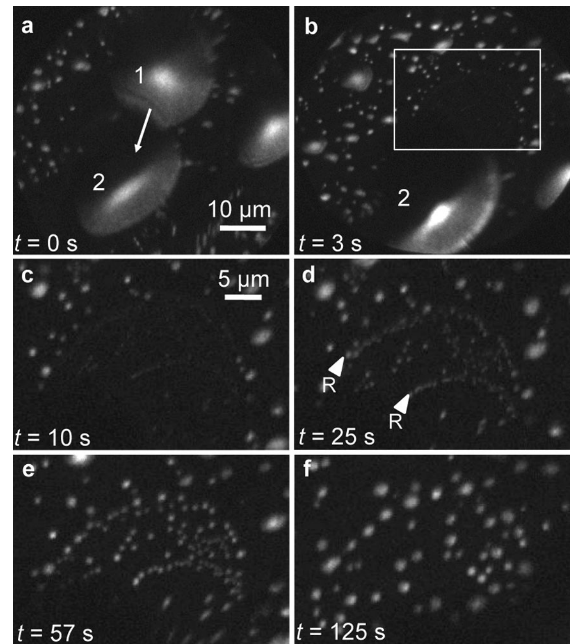

FIG. 1. PEEM images captured from a video (available in the supplementary material [16]) of Ga droplet coalescence at 630 °C. Liquid Ga appears bright against dark GaAs. (a) Droplets 1 and 2 are in close proximity at $t = 0$. (b) At $t = 3$ s, droplet 1 translates across the substrate and coalesces with droplet 2, leaving an exposed substrate arena which is associated with a shallow etch pit. This exposed arena region, enclosed by the frame in (b), is magnified in (c)–(f). Daughter droplet formation (c), and growth (d) is sometimes associated with surface ridges (R).

 © 2010 The American Physical Society

compared such static images with theoretical models for vapor deposition, assuming that Ga generation and droplet nucleation occurs uniformly across the surface. However, our *in situ* real-time videos of evaporation reveal a very different behavior. In Fig. 1(b), droplet 1 of Fig. 1(a) has been absorbed into droplet 2 (which remains stationary). This coalescence event leaves behind a region (a shallow etch pit [7]) which is framed in Fig. 1(b) and magnified in Fig. 1(c). This region serves as the arena in which the subsequent action takes place. Surprisingly, within 2 sec there is a burst of Ga daughter droplet nucleation [Fig. 1(c)] within this arena. The droplets grow rapidly in size [Fig. 1(d)] until at $t = 51$ s they begin to move [19] across the surface [Figs. 1(e) and 1(f)]. The droplets eventually move out of the arena. Such events occur continuously across the surface; a wider view of another event is shown in a separate video (available online [20]).

After the droplets move out of the arena, there is no subsequent nucleation, which indicates that the initial burst of nucleation is not simply due to the absence of nearby droplets acting as Ga sinks. Thus some previously unanticipated mechanism must be at work. To search for the mechanism we turn to mirror electron microscopy (MEM) [19,21]. This imaging mode provides information on surface morphology, which proves key to understanding the droplet behavior. Figure 2 shows MEM images from a video (available in the supplementary material [22]) of a coalescence event and the subsequent evolution. At $t =$ 0 s, droplet 1 is absorbed into droplet 2; the concave etch pit from droplet 1 is clearly visible in Fig. 2(b). In Fig. 2(c), daughter droplets appear and move within this ‘‘arena’’ as in the PEEM video [Figs. 1(e) and 1(f)]. With time, the etch pit planarizes, and only then do the daughter droplets move away from the region as shown in Fig. 2(d). Thus the initial rapid planarization of the depression coincides with the initial formation of daughter droplets, while no further nucleation occurs after the surface is planarized. Moreover, the duration of rapid daughter droplet growth appears to correspond to the time needed for appreciable planarization.

Planarization during crystal evaporation is a well-studied phenomenon with important applications [14]. Typically, in a closed system (Knudsen evaporation) there is some equilibrium population of adatoms (or other mobile species) on the surface. In vacuum, though, the surface loses adatoms by evaporation, and the adatom population is replenished by atoms detaching from atomic steps on the surface [14,15]. The steps therefore recede with time, and for Si (001) under ideal conditions large areas can be swept free of steps and made atomically flat [14].

However, this alone would not explain our burst of nucleation and growth. To understand the novel behavior we construct a simple model for Langmuir evaporation of GaAs. Past work suggests that Ga adatoms persist on the surface long enough to maintain approximate equilibrium

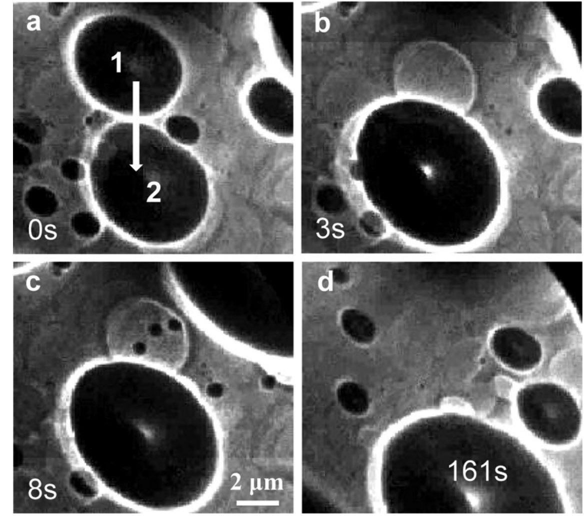

FIG. 2. MEM images captured from a video (in the supplementary material [22]) of Ga droplet coalescence at 650 °C. In this imaging mode, concave surface features such as etch depressions appear bright relative to planar regions and convex droplets appear as dark circles surrounded by a bright concentric ring [19]. (a) At $t = 0$ s, droplet 1 translates across the substrate and coalesces with droplet 2, leaving an exposed bright, circular etch depression region in (b). Note that droplet sizes are exaggerated in MEM and the true size of droplet 1, for example, closely approximates the shallow etch pit in (b). (c) Daughter droplets nucleate in the etch depression and appear as dark circles. (d) Eventually the etch pit planarizes.

between terrace and steps [23], as in Si. However, As evaporates readily, so that in MBE growth a constant excess flux of As is required to prevent decomposition. We therefore assume that, in vacuum at these temperatures, any mobile As surface species evaporates too rapidly to maintain a significant population across the terrace. Then the rate of Ga evaporation is approximately independent of step density, while the rate of As evaporation is approximately proportional to step density. Assuming a standard transition rate model for Ga and As evaporation, the evaporation rates per unit area are

$$F_{\mathrm{Ga}} = r_{\mathrm{Ga}} \exp\left(\frac{\mu_{\mathrm{Ga}} - E_{\mathrm{Ga}}}{kT}\right), \tag{1}$$

$$F_{\mathrm{As}} = r_{\mathrm{As},s} L_s^{-1} \exp\left(\frac{N(\mu_{\mathrm{GaAs}} - \mu_{\mathrm{Ga}}) - E_{\mathrm{As}N}}{kT}\right). \tag{2}$$

Here the chemical potentials of Ga and As on the surface are μ_{Ga} and μ_{As}; the transition state for As evaporation involves N atoms (e.g., $N = 2$ for As dimers), and we have used $\mu_{\mathrm{Ga}} + \mu_{\mathrm{As}} = \mu_{\mathrm{GaAs}}$, where μ_{GaAs} is the bulk crystal free energy per atom pair. E_{Ga} and $E_{\mathrm{As}N}$ are the respective transition state energies for Ga and As evaporation. The rate constants r_{Ga} (per unit area) and $r_{\mathrm{As},s}$ (per unit step length) include the transition state entropy or degeneracy, e.g., density of sites for evaporation. For small deviations

from the (001) orientation, the step density L_s^{-1} varies with miscut angle θ roughly as $L_s^{-1} \approx (L_0^{-2} + h_s^{-2}\theta^2)^{1/2}$, where h_s is the atomic step height, and L_0^{-1} is the step density present even on the facet due to kinetic roughening [24].

Congruent evaporation (equal Ga and As) occurs because the chemical potential self-adjusts. High T favors As evaporation, causing Ga to accumulate on the surface. As a result, μ_{Ga} rises until $F_{\mathrm{Ga}} = F_{\mathrm{As}}$ is restored. However, if the Ga chemical potential rises above the liquidus value $\mu_{\mathrm{Ga},0}$, Ga droplets can nucleate. Their presence tends to pin the chemical potential at $\mu_{\mathrm{Ga}} = \mu_{\mathrm{Ga},0}$. Therefore congruent evaporation breaks down above the congruent evaporation temperature

$$kT_c = \frac{(N+1)\mu_{\mathrm{Ga},0} - N\mu_{\mathrm{GaAs}} - E_{\mathrm{Ga}} + E_{\mathrm{As}N}}{\ln(r_{\mathrm{As},s}/L_s r_{\mathrm{Ga}})}. \quad (3)$$

If droplets pin μ_{Ga} at $\mu_{\mathrm{Ga},0}$, then Eqs. (1) and (2) show that above T_c As evaporates more quickly than Ga, releasing Ga and causing droplets to grow. Below T_c, droplets will shrink and disappear, at which point μ_{Ga} is free to adjust and congruent evaporation is restored.

Above T_c, if droplet coalescence suddenly exposes a region of much higher local miscut, then from Eq. (2), that region will experience much faster As evaporation and Ga release than the surroundings, explaining the burst of nucleation and growth of daughter droplets. This rapid Ga release will continue until the evaporation drives local planarization.

Equation (3) explicitly predicts a dependence of T_c on the morphology, with larger local miscut giving a lower local T_c. This in turn suggests novel possibilities for controlled nanostructure formation on patterned substrates. Evaporation should occur preferentially on sloped regions. Annealing of the surface would allow the spontaneous generation of droplets at predetermined locations. These droplets could then be converted to semiconductor quantum structures under an overpressure of As or other group-V vapor, as in standard droplet epitaxy techniques [9–13], offering a new route to nanostructure fabrication. Annealing at a temperature above the T_c of the sloped regions but below the T_c of the flat regions would give especially robust Ga placement, important for uniformity and reproducibility in technological applications—Ga is released only in the intended high-slope regions, while in the flat regions (where T is below the local T_c) any excess Ga tends to evaporate.

We demonstrate such positioning at a proof-of-concept level in Fig. 3. We first heated a GaAs (001) sample above T_c to form a number of well-separated Ga droplets. The sample was then cooled below T_c so that the Ga droplets shrink [Fig. 3(a)] and eventually disappear [Fig. 3(b)] [19]. This leaves a surface patterned with nanoscale depressions (the droplet etch pits). In Fig. 3(a), droplet 1 is the largest droplet and therefore the last to disappear, leaving the greatest depression. When we slowly increase the temperature to 620 °C, a new droplet is generated at precisely the same position in Fig. 3(c). No other droplets appear on the planar surface or in the other depressions. We can control the stability of the single droplet over a significant time period (many minutes) and temperature range (±5 °C) [Fig. 3(d)]. Increasing the temperature to 635 °C, we see in Fig. 3(e) that an additional droplet appears at the etch pit left by droplet 2 in Fig. 3(a), as expected. Even after 1 min. [Fig. 3(f)], ~90% of the new droplets reappearing correspond to previous etch pit positions. This demonstrates that position-controlled droplets can be readily generated from ''patterned'' surface features.

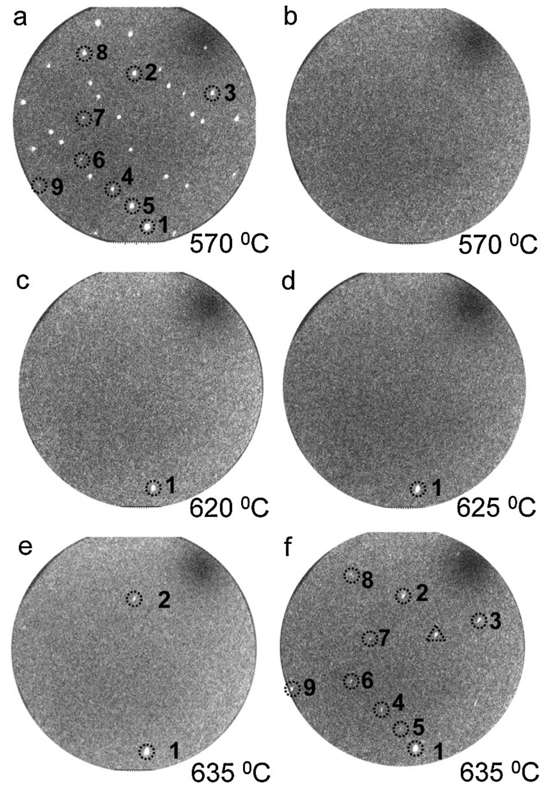

FIG. 3. PEEM images of Ga droplet shrinkage and formation. (a) The sample is cooled below T_c so that Ga droplets gradually shrink until they all eventually disappear in (b). Circled droplet 1 in (a) is the largest droplet and the last to disappear. On slowly heating the sample to 620 °C, a new droplet is generated in the original position of droplet 1 (c). (d) This droplet was observed to be stable in the temperature range of 620–625 °C for several minutes with no other droplets appearing. (e) Increasing the temperature to 635 °C results an additional droplet appearing at the original position of droplet 2 in (a). (f) After a further minute at 635 °C, ~90% of the new droplets reappearing correspond to previous droplet positions in (a) (circled droplets). The droplet enclose by a triangle has appeared at a new position.

We expect that capillary effects may also play a role in our observations. Concave regions are energetically favorable for the liquid droplets, providing an extra force acting to position the droplets on a patterned substrate. Indeed, many of the droplets initially appear in strings in Fig. 1(d),

associated with ridges within the etch pit, which might reflect capillary effects. However, we do not observe droplet formation on preexisting surface features such as ridges located away from coalescing parent drops, indicating that enhanced Ga release is an important contribution to droplet formation. We therefore expect both capillarity and enhanced Ga release contribute to the formation and positioning of droplets in Fig. 3.

Different GaAs surfaces such as (111)*A* and *B* have different atomic structures for the terrace and steps. Therefore the kinetic parameters in Eq. (3) will be different for each surface. Equation (3) then predicts that each surface will have a different T_c [3] as well as a different dependence on miscut.

In conclusion, we have shown that evaporation and surface morphology are mutually connected during Langmuir evaporation of GaAs (001). A simple model of GaAs evaporation, in which the rate of As evaporation depends on the step density, explains the striking bursts of daughter droplet nucleation. Most significantly, the model predicts a morphology dependent congruent evaporation temperature, which is consistent with our *in situ* surface electron microscopy studies of droplet regeneration at etch pits. This basic concept and proof-of-principle demonstration have important technological implications for the self-assembly and positioning of quantum structures on surfaces by combining lithography with droplet epitaxy.

D. E. J and W. X. T. acknowledge support by the Australian Research Council (Grant No. DP0985290). We thank Rod Mackie for technical support.

*tersoff@us.ibm.com
†david.jesson@monash.edu

[1] C. T. Foxon, J. A. Harvey, and B. A. Joyce, J. Phys. Chem. Solids **34**, 1693 (1973).
[2] J. R. Arthur, J. Phys. Chem. Solids **28**, 2257 (1967).
[3] B. Goldstein, D. J. Szostak, and V. S. Ban, Surf. Sci. **57**, 733 (1976).
[4] J. Y. Tsao, *Materials Fundamentals of Molecular Beam Epitaxy* (Academic Press, San Diego, 1993).
[5] C. Chatillon and D. Chatain, J. Cryst. Growth **151**, 91 (1995).
[6] M. Zinke-Allmang, L. C. Feldman, and W. van Saarloos, Phys. Rev. Lett. **68**, 2358 (1992).
[7] T. D. Lowes and M. Zinke-Allmang, J. Appl. Phys. **73**, 4937 (1993).
[8] N. Isomura, S. Tsukamoto, K. Iizuka, and Y. Arakawa, J. Cryst. Growth **301–302**, 26 (2007).
[9] T. Mano, T. Kuroda, S. Sanguinetti, T. Ochiai, T. Tateno, J. Kim, T. Noda, M. Kawabe, K. Sakoda, G. Kido, and N. Koguchi, Nano Lett. **5**, 425 (2005).
[10] M. Yamagiwa, T. Mano, T. Kuroda, T. Tateno, K. Sakoda, G. Kido, N. Koguchi, and F. Minami, Appl. Phys. Lett. **89**, 113115 (2006).
[11] S. Huang, Z. Niu, Z. Fang, H. Ni, Z. Gong, and J. Xia, Appl. Phys. Lett. **89**, 031921 (2006).
[12] C. Somaschini, S. Bietti, N. Koguchi, and S. Sanguinetti, Nano Lett. **9**, 3419 (2009).
[13] J. H. Lee, Z. M. Wang, Z. Y. AbuWaar, and G. J. Salamo, Cryst. Growth Des. **9**, 715 (2009).
[14] D. Lee and J. Blakeley, Surf. Sci. **445**, 32 (2000).
[15] W. K. Burton, F. Cabrera, and F. C. Frank, Phil. Trans. R. Soc. A **243**, 299 (1951).
[16] See supplementary material at http://link.aps.org/supplemental/10.1103/PhysRevLett.105.035702 for the PEEM video from which Fig. 1 is taken, showing Ga droplet coalescence and subsequent nucleation of daughter droplets.
[17] J. Massies, P. Etienne, F. Dezaly, and N. T. Linh, Surf. Sci. **99**, 121 (1980).
[18] C. Norris and J. T. M. Wotherspoon, J. Phys. F **7**, 1599 (1977).
[19] J. Tersoff, D. E. Jesson, and W. X. Tang, Science **324**, 236 (2009).
[20] See supplementary material at http://link.aps.org/supplemental/10.1103/PhysRevLett.105.035702 for a wider-view PEEM video of Ga droplet coalescence and subsequent nucleation of daughter droplets.
[21] S. A. Nepijko, N. N. Sedov, and G. Schönhense, J. Microsc. **203**, 269 (2001).
[22] See supplementary material at http://link.aps.org/supplemental/10.1103/PhysRevLett.105.035702 for the MEM video from which Fig. 2 is taken, showing Ga droplet coalescence and subsequent nucleation of daughter droplets.
[23] J. Tersoff, M. D. Johnson, and B. G. Orr, Phys. Rev. Lett. **78**, 282 (1997).
[24] P. Nozières and F. Gallet, J. Phys. (Paris) **48**, 353 (1987).